Oncogene (1997) 15, 2037–2048

Retinoic acid and the cyclin dependent kinase inhibitors synergistically alter proliferation and morphology of U343 astrocytoma cells

Peter B Dirks[1,2], Ketan Patel[1], Sherri Lynn Hubbard[1], Cameron Ackerley[2], Paul A Hamel[2] and James T Rutka[1,2]

[1]Division of Neurosurgery, Hospital for Sick Children, Toronto, Ontario, M5G 1X8 and [2]Department of Pathology, University of Toronto, Toronto, Ontario, M5S 1A8, Canada

We have characterized the expression and activity of the cell cycle regulatory machinery and the organization of the cytoskeleton of the p16^{Ink4a}-deficient astrocytoma cell line, U343 MG-a (U343), following retinoic acid (RA) treatment. RA causes cell cycle arrest at low cell density and significant morphological changes in U343 cells, reflected by reorganization of the intermediate filament, GFAP, and actin. RA-induced cell cycle arrest is also associated with induction of p27^{Kip1} expression, inhibition of cdk2-associated kinase activity and alteration of the phosphorylation state of the pRB-family proteins. We next determined the effect of inducing expression of the cyclin dependent kinase inhibitors (CKI's), p16^{Ink4a}, p21$^{Cip1/Waf1}$ or p27^{Kip1} on the proliferation and morphology of these malignant astrocytoma cells in the absence and presence of RA. Induction of p16, p21 or p27, using the tetracycline repressor system, potently inhibits proliferation of U343 cells. However, rather than resembling RA-treated cells, CKI-induced U343 cells become flat with abundant cytoplasm and perinuclear vacuolization. CKI-induced morphological alterations are accompanied by a significant reorganization of glial filaments within the cytoplasm. Interestingly, when U343 cells are growth arrested by p16, p21 or p27 induction and treated simultaneously with RA, a dramatic morphological change occurs, cells acquiring multiple long, tapering processes reminiscent of primary astrocytes. This rearrangement is accompanied by reorganization of GFAP, vimentin and actin. Vimentin specifically relocalizes to the tips of the long processes which form. The arrangement of intermediate filaments in these cells is, in fact, indistinguishable from their arrangement in primary human astrocytes. These data demonstrate that when a strong proliferative block, produced by CKI expression, occurs in conjunction with the morphogenic signals generated by RA, these p16-deficient malignant astrocytoma cells are induced to phenotypically resemble normal astrocytes.

Keywords: Astrocytoma; cyclins; cyclin-dependent kinases; GFAP; retinoic acid; p16; p21

Introduction

Progression through the G_1 phase of the cell cycle is controlled, in part, by the regulation of activity of cyclin-dependent kinases (cdk's) (for review, see Weinberg, 1995). One important means of regulating cdk activity occurs through the formation of complexes comprised of the cdk's and the cyclin-dependent kinase inhibitors (CKI's). The activities of these CKI's include binding to cyclin/cdk co-complexes and inhibition of their associated kinase activity (for review, see Sherr and Roberts, 1995), binding to specific cdks and subsequent inhibition of their association with cyclins (Parry *et al*., 1995) and, paradoxically, promotion of the formation of some cyclin-cdk complexes (LaBaer *et al*., 1997). So, for example, in response to DNA damage, p53 induces expression of the CKI protein, p21$^{Cip1/Waf1}$ (p21), leading to inhibition of activity of multiple cyclin/cdk co-complexes (Dulic *et al*., 1994; El-Deiry *et al*., 1993; Harper *et al*., 1993; Waldman *et al*., 1995). p27^{Kip1} (p27) contributes to the growth suppressive signals from TGF-β or cell-cell contact (Hengst *et al*., 1994; Polyak *et al*., 1994a,b; Reynisdottir *et al*., 1995; Toyoshima and Hunter, 1994) and inhibition of its expression by antisense oligonucleotides prevents G_1 arrest in response to mitogen depletion (Coats *et al*., 1996). The importance of p27 in regulating cell growth has recently been appreciated from studies which examined the phenotype of mice deficient for this CKI (Fero *et al*., 1996; Kiyokawa *et al*., 1996; Nakayama *et al*., 1996). Mice nullizygous for p27 exhibit hyperplasia in multiple organ systems due to failure to exit the cell cycle during terminal differentiation. The loss of p27 is also associated with neoplastic transformation of the pituitary gland, consistent with the notion that p27 functions as a tumor suppressor.

Loss of another CKI, p16^{Ink4a} (p16), has also been implicated in malignant transformation (Kamb *et al*., 1994; Serrano *et al*., 1993, 1996). Although not associated with the generalized hypertrophy of the p27 knock-out mice, p16-deficient mice exhibit a number of soft tissue sarcomas and are highly susceptible to radiation and carcinogen-induced tumors (Serrano *et al*., 1996). Loss of p16 expression has also been implicated in human cancers due to its high frequency of deletion or mutation in melanomas, pancreatic adenocarcinomas, leukemias and malignant astrocytomas (Caldas *et al*., 1994; Hussussian *et al*., 1994; Ichimura *et al*., 1996; Jen *et al*., 1994; Kamb, 1995; Kamb *et al*., 1994; Liu *et al*., 1995; Schmidt *et al*., 1994).

We have been studying cell cycle regulatory pathways in the p16-deficient, malignant astrocytoma cell line, U343 MG-A (U343). Retinoic acid (RA) treatment of these cells inhibits proliferation, alters morphology, and increases the expression and organization of a marker of glial differentiation, glial

Correspondence: JT Rutka
Received 7 March 1997; revised 30 June 1997; accepted 30 June 1997

fibrillary acidic protein (GFAP) (Rutka *et al*., 1988). In the present study, we sought to determine the relationship between RA-induced differentiation and the expression of several key cell cycle regulators. We show that whereas both CKI-induction and RA treatment can independently cause U343 cells to arrest in G_1 phase, the cell morphologies resulting from each treatment are markedly different. Our data demonstrate further that when p16-, p21- or p27-induced cell cycle arrest is accompanied by RA treatment, a profound phenotypic change in U343 astrocytoma cells occurs, cells becoming morphologically indistinguishable from primary astrocytes.

Results

Retinoic acid alters the morphology and growth characteristics of U343 cells

The p16-deficient, human astrocytoma cell line U343 responds to all-trans RA treatment (Rutka *et al*., 1988). Figure 1 shows that RA inhibits U343 proliferation (Figure 1a) and induces morphological changes (Figure 1b–c). So, rather than the tightly packed 'cobble-stone' appearance of untreated cells (Figure 1b), RA causes cells to elongate and acquire a somewhat bipolar appearance (Figure 1c). Occasional long processes (<10% of cells) are also observed in these RA treated cultures. The altered morphology in RA-treated U343 cells is accompanied by changes in cytoskeletal protein assembly (Figure 2). For example, untreated U343 cells exhibit diffuse cytoplasmic and prominent perinuclear cytoplasmic staining for GFAP (Figure 2a). This disorganized pattern of expression is replaced by a filamentous arrangement of GFAP staining in the cytoplasm and processes of RA-treated cells (Figure 2b). The RA-induced reorganization of GFAP is also accompanied by changes in its apparent phosphorylation state. Using a phospho-GFAP-specific monoclonal antibody, YC-10, which recognizes phosphoserine in the context of a ten amino acid peptide of the GFAP amino-terminus (Matsuoka *et al*., 1992; Yano *et al*., 1991), we show that a prominent punctate or speckled staining pattern is evident both in the cytoplasm and the nucleus of untreated cells (Figure 2c–d). This punctate staining pattern is lost in the cytoplasm but not in the nucleus of U343 cells treated with RA. Thus, RA-induced reorganization of the U343 astrocytoma cytoskeleton is accompanied by a loss of the phosphorylated form of GFAP from the cytoplasm.

RA treatment alters the expression and activity of cell cycle regulatory proteins

We next determined if the G_1 arrest following RA treatment is accompanied by changes in the expression

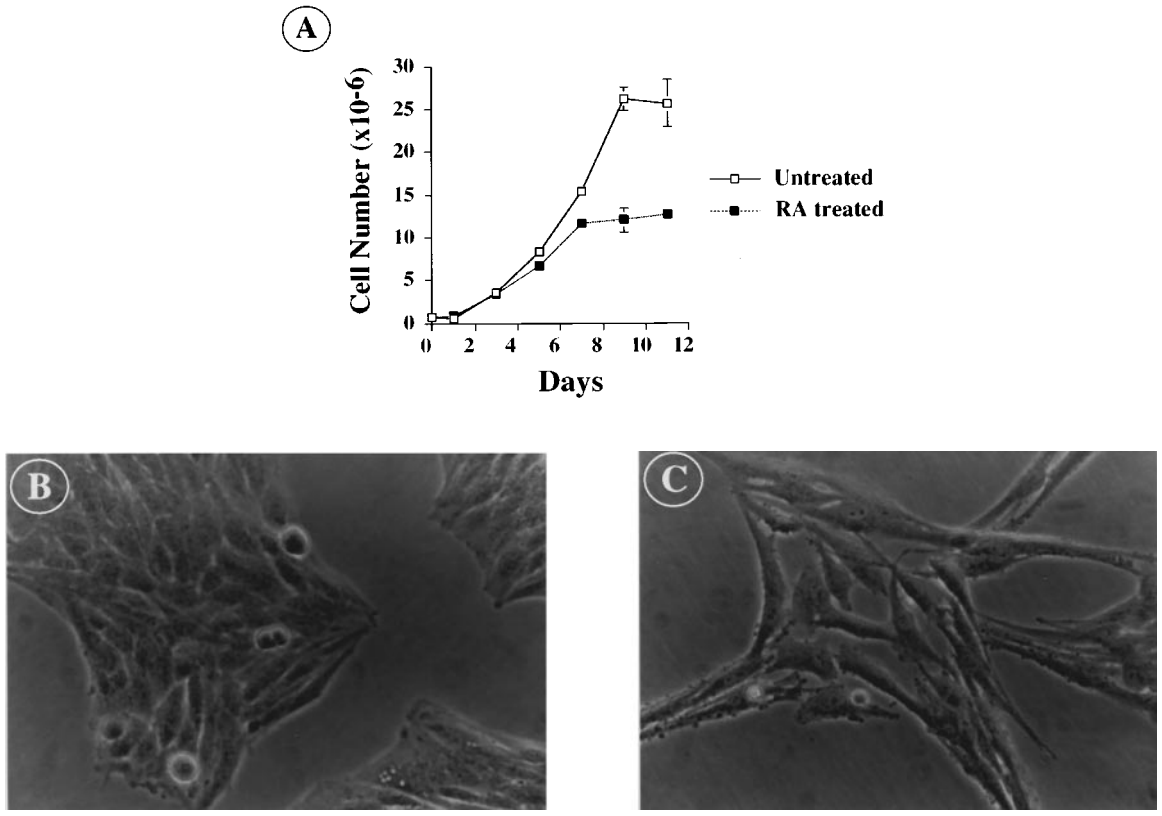

Figure 1 Growth of U343 cells in the presence and absence of retinoic acid. (**a**) Growth curve analysis of U343 astrocytoma cells treated in the presence or absence of 5×10^{-6} M RA-treated astrocytoma cells show a decrease in cellular proliferation beginning on day 3 compared to controls. The difference in cell number between control and RA-treated cultures is maximum by day 9. (**b**, **c**) Morphological alterations induced by RA treatment of U343 astrocytoma cells. Control U343 cells show colonies with polygonal cells and marked cell crowding (**b**) In contrast, there is a distinct morphological change brought about by RA treatment. RA-treated cells are predominantly bipolar with extension of slender, tapering cell processes (**c**) Cell crowding and colony formation are not observed. **b**–**c**, phase microscopy, ×300

and activity of cell cycle regulatory factors, specifically, the G_1 cyclins, their associated kinases and kinase inhibitors (Figure 3). The steady state protein levels of cdk1, cdk2, cdk4, and cdk6 do not change with RA treatment. In the case of the CKI, p21, induction occurs with slightly increased kinetics in RA-treated relative to untreated U343 cells. In contrast, expression of p27 is fivefold higher in day 5 RA-treated cells compared to untreated U343 cells. This level of p27 in day 5 RA-treated cells is reached in untreated cells only after day 9 where proliferation of these cells has slowed (data not shown). Following RA treatment, cyclin D1 protein shows no change whereas cyclins A and E gradually decrease (data not shown).

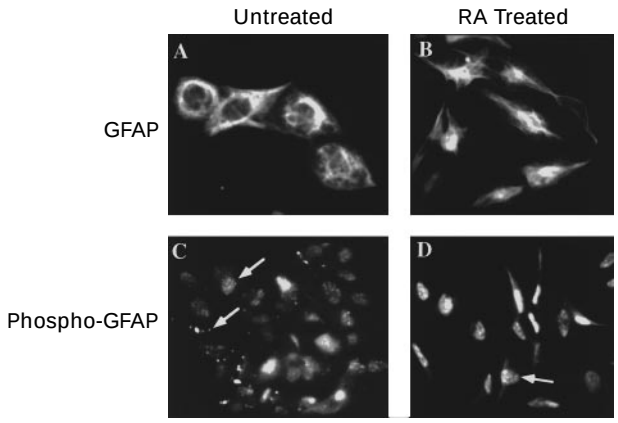

Figure 2 RA-induced rearrangement of the U343 astrocytoma cytoskeleton. (**a**) Control U343 cells show hazy perinuclear staining for GFAP (nonphospho-specific) in polygonal cells. Immunofluorescence microscopy, ×780. (**b**) RA-treated cells have a prominent network of glial filaments stained for GFAP. These filaments bridge the cytoplasmic space from the nucleus to the plasma membrane and appear far more organized than are filaments in control cells. (**c**) Staining for phospho-GFAP reveals a punctate cytoplasmic and nuclear pattern of staining (arrows) in untreated U343 cells. (**d**) RA-treated cells are characterized by a complete disappearance of the cytoplasmic pattern of staining but preservation of nuclear staining. **b**–**d**, immunofluorescence microscopy, ×630

The altered kinetics of p27 induction following RA treatment suggested that the kinase activity associated with the cdk's would also be inhibited in U343 cells. Thus, cdk2 or cdk4 were immunoprecipitated from RA-treated or untreated U343 cells. Their associated kinase activity was then determined in *in vitro* kinase assays using histone H1 or purified human recombinant full length pRB, respectively, as substrates. As the right panels in Figure 3 demonstrate, the kinase activity associated with cdk2 is strongly inhibited by day 5 of RA treatment, the point at which both p21 and p27 are strongly induced. In the case of cdk4, however, only a minor but consistent reduction in its associated kinase activity is seen in these RA-treated cells. Thus, the proliferative block induced in U343 cells appears to be associated with p21 and p27 induction and a commensurate inhibition of cdk2, but not cdk4, associated kinase activity. This block is associated with a morphological change in U343 cells

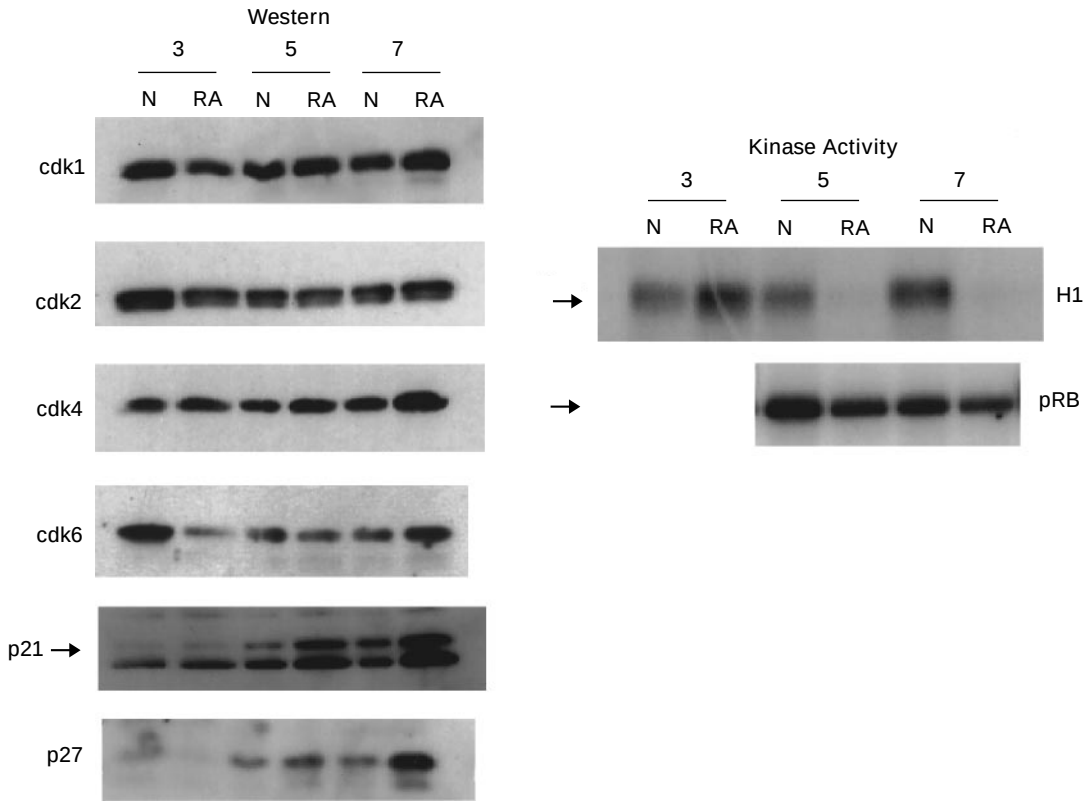

Figure 3 Expression and activity of cell cycle regulatory factors in U343 cells. (Left panel) Western analysis of cdk1, cdk2, cdk4, cdk6, p21, p27 and pRB in untreated and RA-treated U343 cells. p21 and p27 are significantly increased in RA-treated cells on days 5 and 7 relative to untreated cells while cdk levels are unchanged following RA treatment. Only a minor change in the phosphorylation state of pRB is observed in these cells, both hyper- and hypo-phosphorylated forms persisting in untreated and RA-induced cells. (Right panel) Kinase activity of cdk2 and cdk4 in untreated and RA-treated cells. *In vitro* kinase assays demonstrate that cdk2-associated kinase activity is absent by day 5 in RA-treated cells. In contrast, only a small but consistent decrease in cdk4-associated kinase activity is seen with RA treatment

which is distinct from untreated cells and from normal astrocytes.

Effect of induced CKI expression on U343 astrocytomas

The morphological changes and cell cycle arrest caused by RA were associated with induction of p21 and p27. We wished, therefore, to determine if CKI-induced cell cycle arrest would also alter U343 cell morphology and would affect the outcome of RA treatment. Thus, p16, p21 and p27 under the control of the tetracycline-repressor (tet^R) expression system (Gossen and Bujard, 1992; Resnitzky *et al*., 1994) were individually introduced into U343 cells. Several lines were isolated where tight tetracycline-dependent control of CKI expression could be demonstrated. All of the lines for each CKI behaved identically and a representative line for each is presented in Figure 4.

Figure 4a, c and e demonstrate the regulated expression of p16, p21 and p27, respectively, using the tet^R system. For all three CKI's little or no detectable expression is seen under repressed condi-

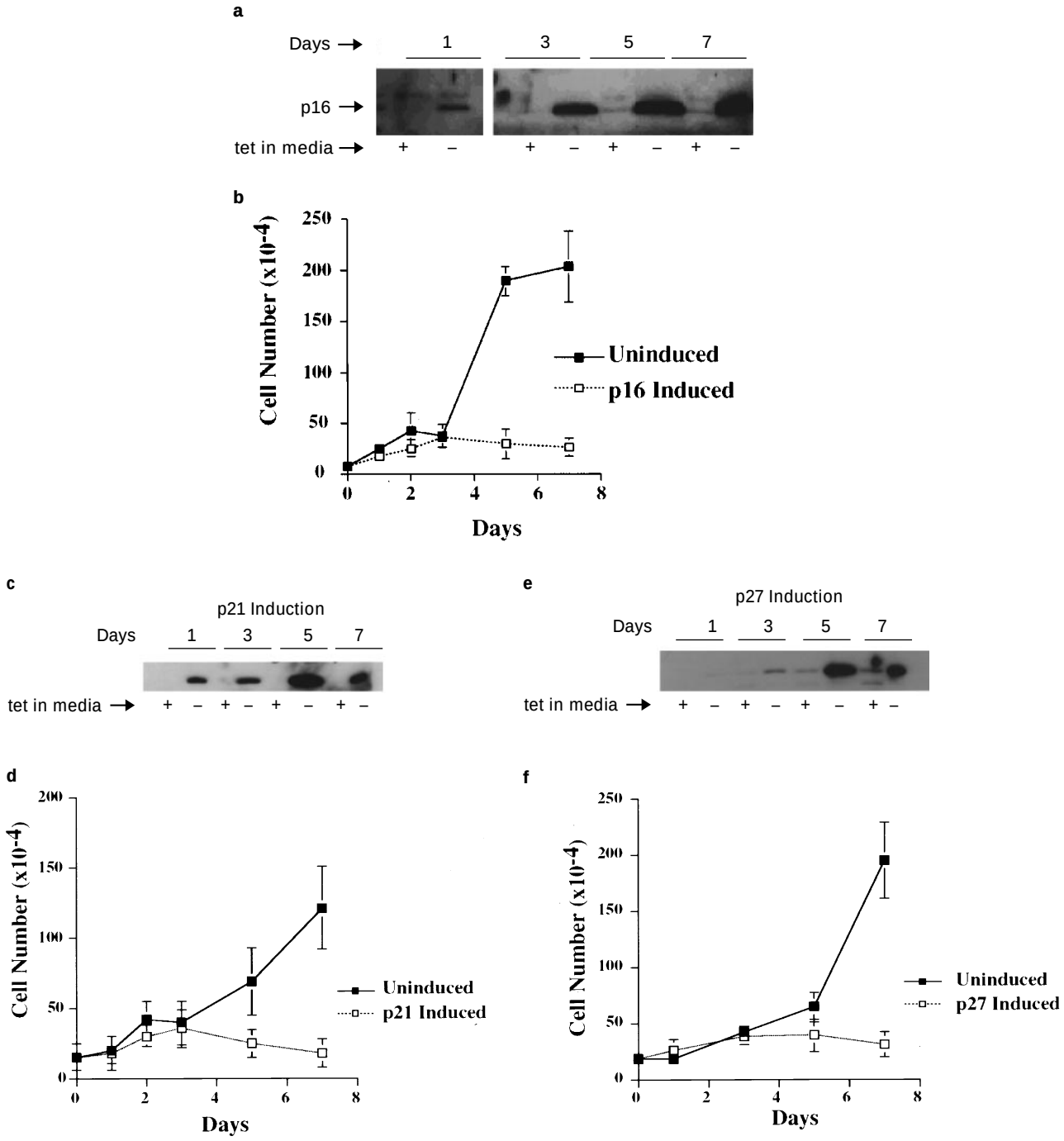

Figure 4 Tetracycline-inducible expression of CKI's in U343 cells. U343 cells with CKI's under the control of the tetO were grown in the presence (+) or absence (−) of tetracycline (tet). (**a**) Western analysis demonstrates that removal of tet from the media causes a strong induction of p16 protein by 24 h which increases progressively over several days achieving maximal levels by day 5. Uninduced U343 cells express little p16 demonstrating the tight control of expression with this system. Induction of p16 causes a potent proliferative block as demonstrated by growth curve analysis (**b**). Similarly, induction of p21 or p27 (**c**, **e**) causes growth arrest of U343 cells as determined by growth curves analysis (**d**, **f**)

tions (+). In contrast, within 24 h of removing tet(−), expression of all three CKI's can be detected. Expression reached maximal levels for all three CKI's near day 5 following induction. As expected, expression of p16, p21 or p27 produced a potent proliferative block in U343 cells (Figure 4b, d and f, respectively). In all three cases, no increase in cell numbers were observed after day three following removal of tet. Table 1 demonstrates further that by day 5, the majority of the cells are blocked in G_1 in the p16 and p27 arrested cells. In the case of p21, we consistently observe that a significant fraction of these cells are arrested in the G_2/M portion of the cell cycle.

Table 1 Flow cytometric analysis of tetracycline induced and uninduced U343 cells after 3 days of experiment

	%G1	*%S*	*%G2M*
p16 OFF	71	18	11
p16 ON	95	2	3
p21 OFF	75	12	13
p21 ON	88	3	9
p27 OFF	69	20	11
p27 ON	93	3	4

We next determined the effect of CKI induction on the expression and activity of factors influenced by the CKI's, specifically the cdk's, the pRB- and the E2F-family proteins. Figure 5a illustrates the expression pattern of cell cycle regulatory proteins during p16 induction. The three pRB-family proteins, pRB, p107 and p130 are primarily hyperphosphorylated in uninduced cells (day 0) but are found exclusively in their hypophosphorylated forms by day 3 of p16 induction. Additionally, pRB and, more dramatically, p107 are reduced in levels in these cells while p130 is induced as p16 expression increases. E2F-1, which like p107 and pRB contain E2F-binding sites in their promoter regions (Shan *et al*., 1994), is strongly repressed following p16 expression. In contrast, E2F-4, which is the predominant E2F-family member associated with p130 in quiescent cells (Cobrinik *et al*., 1993; Smith *et al*., 1996; Vairo *et al*., 1995), increases slightly in these cells.

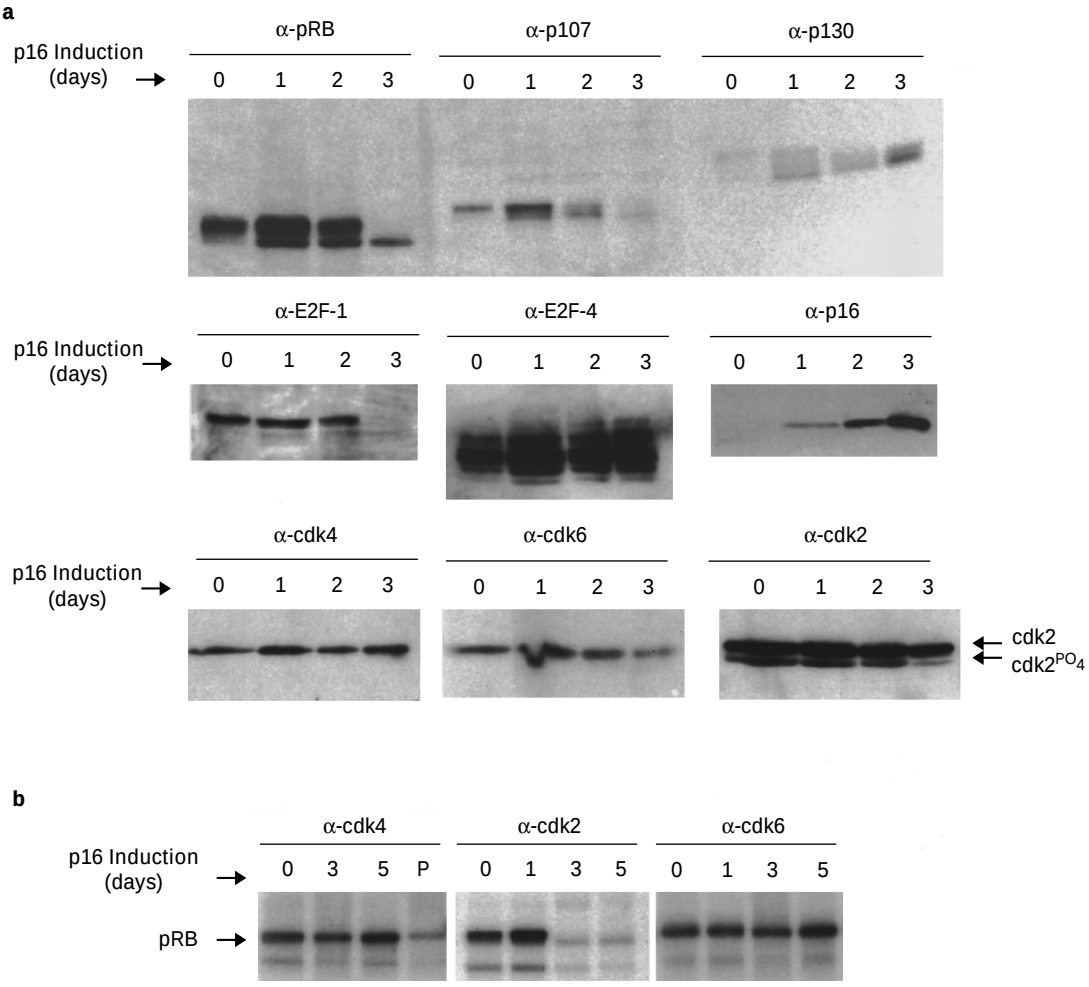

Figure 5 Expression and activity of factors regulated by CKI's. (**a**) Coincident with strong induction of p16, there is a decrease in expression of pRB and p107, with shift to the hypophosphorylated form. p130 is also shifted from four identifiable forms to two hypophosphorylated forms but its levels are increased as p16 is induced. E2F-1 protein is also decreased to almost undetectable levels while E2F-4 levels remain constant. Western blot analysis for cdk2, cdk4 and cdk6 showed little variation in steady state levels of these proteins following p16 induction. The Western blot for cdk2 reveals a loss of the active, hyperphosphorylated form of cdk2 (lower band) and shift exclusively to the slower migrating, hypophosphorylated form. (**b**) Kinase activity associated with cdk2, cdk4 and cdk6. As expected, cdk2 shows a strong decrease in the associated kinase activity as cells become growth arrested. In contrast, we consistently observe little change in the kinase activity associated with cdk4 and cdk6. The level of non-specific kinase activity for cdk4 was confirmed by addition of a blocking peptide (lane P)

The bottom row of Western blots in Figure 5a demonstrates that little change in the levels of cdk2, cdk4 and cdk6 occur in these p16-arrested cells. Cdk2 does, however, undergo a significant change in mobility in SDS–PAGE. Specifically, in exponentially growing p16-deficient cells (day 0), cdk2 migrates as two species, a faster migrating, hyperphosphorylated form, which is the active form of cdk2 and a slower, inactive hypophosphorylated form (Poon and Hunter, 1995). When U343 cells become arrested following expression of p16, the active, hyperphosphorylated form of cdk2 is lost. It should be noted further that neither p21 or p27 were induced in the p16-arrested cells (data not shown). The kinase activity associated with cdk2, cdk4 and cdk6 were also determined (Figure 5b). As expected, cdk2 shows a strong decrease in the associated kinase activity as cells become growth arrested. In contrast, we consistently observe little change in the kinase activity associated with cdk4 and cdk6. The same antibodies for cdk4 and cdk6 detected changes (decreased) in associated kinase activity for these two cdk's when isolated from exponentially growing and differentiated myoblasts (C_2C_{12} cells). The persistence of cdk4-associated kinase activity in these cells was also verified using three independent antibodies (data not shown).

The phosphorylation state of the pRB-family proteins is also altered in the p21 and p27-induced cells. A representative Western for pRB is seen in Figure 6a. Like the cells where p16 is induced, pRB becomes primarily hypophosphorylated and its levels repressed following p21 or p27 induction. The kinetics of this transition for the p21/p27-induced cells is slightly delayed relative to effects induced by p16. p107 levels are also repressed following both p21 and p27 induction. In the case of p130, p21-expressing cells have increased levels of p130 while little change in p130 was observed in p27-arrested cells. As with p16-induced cells, expression of E2F-1 was sharply reduced and E2F-4 levels were unchanged in p27 and p21-induced cells (data not shown). For p27-arrested cells, the kinase activity associated with cdk2 and cdk4 is similar to that observed for cells arrested following p16 expression (data not shown).

CKI expression during RA-stimulation induces unique morphological and cytoskeletal changes in U343 astrocytomas

The cell cycle arrest associated with p16, p21 or p27 induction in U343 astrocytomas is accompanied by a strong morphological transition. All three CKI's induced identical morphological and cytoskeletal alterations and these changes could be reversed by repressing CKI expression by adding tet back to the media. Figure 7 illustrates the gross morphological changes associated with CKI expression, p16 used here as an example. Figure 7a shows the usual 'cobble-stone' appearance of U343 cells when p16 expression is repressed. Following p16 expression, however, the cells flatten and contain abundant cytoplasm which has a large number of vacuoles around the nucleus. These 'pancake'shaped cells are in marked contrast to the elongated cells observed following RA-dependent cell cycle arrest (see Figure 7c). We next wished to determine if the CKI-arrested cells, when treated simultaneously with RA, would resemble cells treated with RA exclusively. As Figure 7d illustrates, the combination of a strong proliferative block imposed by p16 in the presence of RA stimulation caused a unique morphological transition. Rather than elongate into cells with a bipolar appearance, these p16-induced,

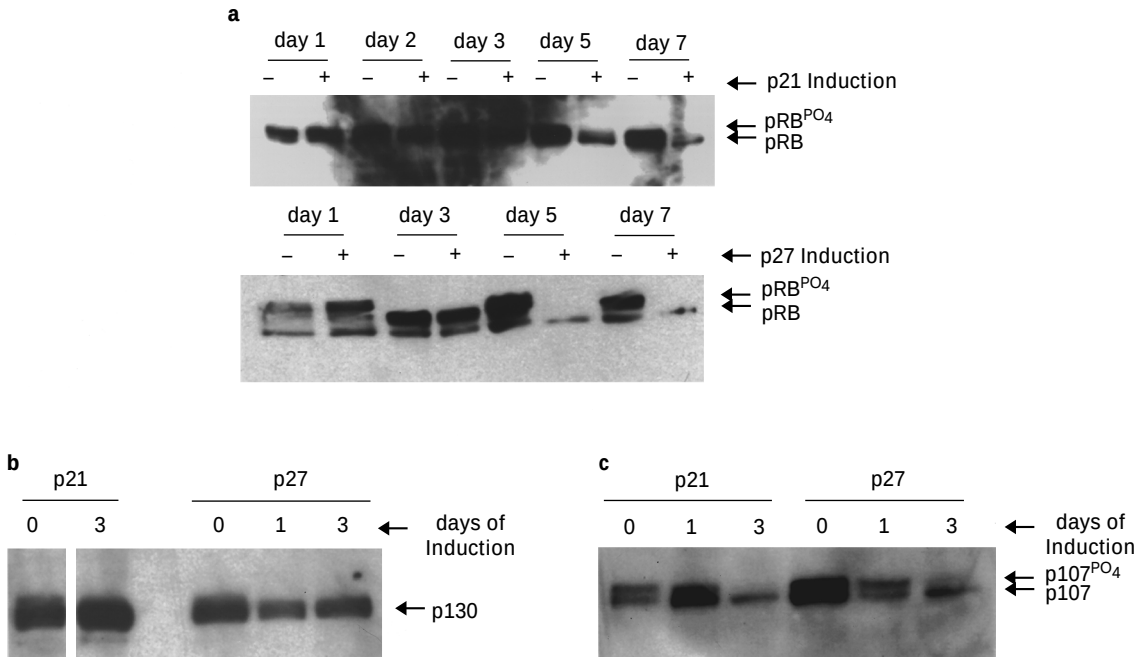

Figure 6 Expression of the pRB-family proteins in p21 and p27 induced U343 cells. (**a**) Induction of p21 or p27 induces a quantitative shift of pRB to its active hypophosphorylated form and a reduction in its overall levels. The kinetics of this transition for the p21/p27-induced cells is slightly delayed relative to effects induced by p16. (**b**, **c**) p107 levels are also repressed for following both p21 and p27 induction. In the case of p130, p21-expressing cells have increased levels of p130 while little change in p130 was observed in p27 arrested cells

RA-treated cells formed numerous long processes. These processes migrated in many directions and typically made contacts with other processes and cell bodies in the dish. These cells, in fact, resembled the morphology of primary astrocytes grown in culture. The same morphological changes shown in Figure 7 for p16 were seen in U343 cells expressing p21 and p27, either alone or in conjunction with RA treatment. Under all of these conditions, cells were viable for greater than 21 days and these effects were reversible after as long as 14 days following CKI-induction/RA-treatment (data not shown). The return to the usual appearance and proliferative state of U343 cells was not accompanied by any obvious increase in cell death.

The profound morphological changes associated with CKI induction and simultaneous RA treatment indicated that important alterations in the U343 cytoskeleton had occurred. We first examined the expression of the glial/astrocyte-specific protein, glial fibrillary acid protein (GFAP; Figure 8). In proliferating U343 cells, this intermediate filament is highly disorganized, appearing as a diffuse, cytoplasmic factor. Induction of the CKI's (p21 in this case), clearly results in an altered arrangement of GFAP (Figure 8, middle panel). The 'pancake' appearance of these cells can easily be appreciated and a fine filamentous arrangement of GFAP radiating outward is observed. When the U343 cells are arrested with p21 and treated with RA, GFAP acquires a distinct arrangement. Under these conditions, a filamentous pattern is still evident in the cell bodies, but GFAP also shows very strong localization to the long processes that have formed under these conditions (Figure 8, lower panel). This figure also illustrates the parallel arrangement of processes that are often seen in these cultures.

We next examined the expression of actin and the intermediate filament protein, vimentin (Figure 9). As with the pattern of staining for GFAP, both vimentin (green) and actin (red) show diffuse, disorganized staining patterns in U343 astrocytomas (Figure 9a). p16 induction (Figure 9b) causes a strong rearrangement of actin, the radial staining pattern reminiscent of GFAP in these same cells, while vimentin only shows limited organization. RA treatment (Figure 9c) causes reorganization of both actin and vimentin, well defined filaments clearly visible for both of these proteins. Figure 9d reveals, however, that a profound rearrange-

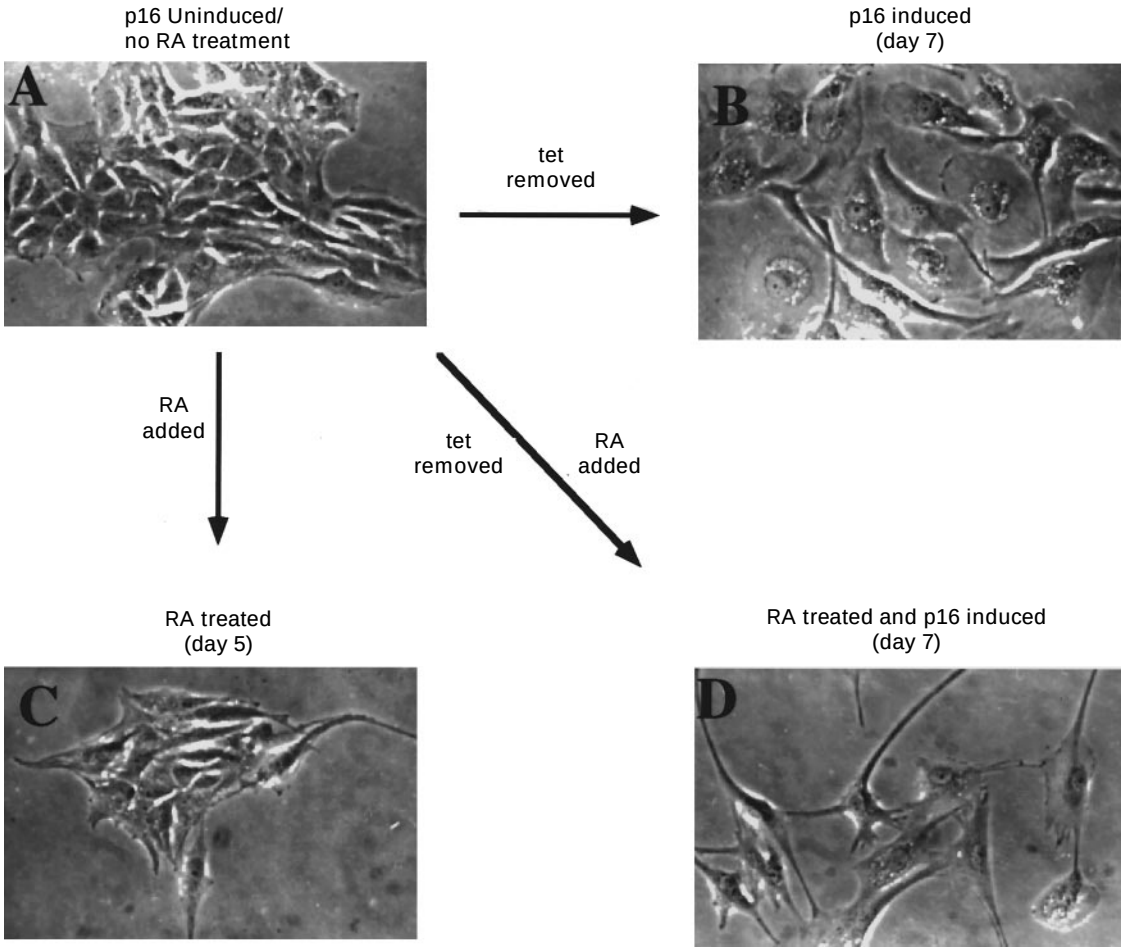

Figure 7 Effects of p16 expression and retinoic acid treatment on U343 cell morphology. Untreated U343 cells (**a**) grow tightly packed in colonies and rarely have any processes. This phenotype is identical to the growth characteristics of the parental U343 cell line. Following 5 days of treatment with all-trans retinoic acid (**c**), U343 cells undergo a phenotypic change consisting of bipolar cell process formation, with short tapering processes and occasional (<10%) long process formation. p16-mediated growth arrest (**b**) is associated with formation of large flat cells with perinuclear vacuolization. Both phenotypes seen in (**b**) and (**c**) are reversible following removal of retinoic acid or suppression of p16, respectively. Panel (**d**) shows that combining retinoic acid treatment with p16 induction, in any order, results in the formation of cells with long processes which contact other cells, morphologically reminiscent of primary astrocytes. p21 and p27 induction with RA treatment had identical effects. Phase microscopy, ×300

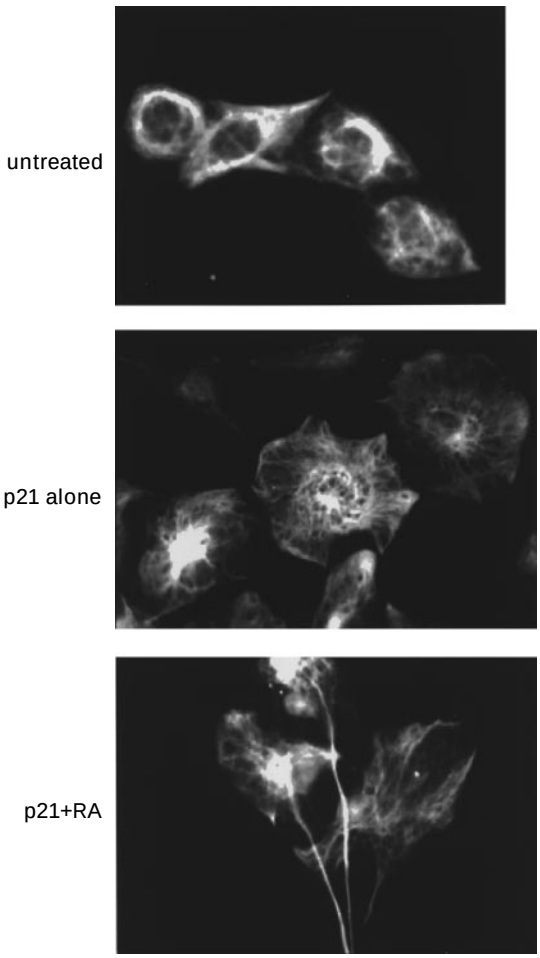

Figure 8 Rearrangement of GFAP in CKI-expressing U343 cells. U343 cells expressing p21 are shown stained for GFAP. An extensive filamentous pattern is seen in these large, flat cells relative to untreated cells. Following p21 expression and RA treatment, GFAP staining reveals the dramatic morphological changes of malignant U343 cells. Cells form many long processes, these processes often migrating in the same direction and in bundles. The processes also form contacts with other cells or processes. The phenotypic changes described here for p21 induction in the presence and absence of RA are identical to the changes observed following p16 or p27 expression in the presence or absence of RA. Immunofluorescence microscopy, ×780 (top), ×630 (middle and bottom)

ment of both actin and vimentin occur in p16 induced cells treated simultaneously with RA. Specifically, fine actin filaments are seen extending into the long processes that form in these cells. More dramatically, the vimentin signal, which was originally confined to the cytoplasm in a perinuclear pattern, is now observed at the tips of the processes of these cells. Vimentin is also localized to a region in the cell body in these RA treated, p16-arrested astrocytomas, this localization being apparently discontinuous with the vimentin at the tips of the processes. The pattern of staining for vimentin and actin in p16-induced, RA-treated U343 cells is more interesting given their staining pattern in normal, primary human astrocytes (Figure 9e). In the astrocytes, vimentin is also localized to the tips of the processes which extend from the cell bodies and, discontinuously, in the cytoplasm in a discrete area. Actin is also highly organized in astrocytes, filaments seen extending into the long processes. These data suggest that the malignant astrocytoma, U343 can be induced to phenotypically resemble quiescent primary human astrocytes only when a potent proliferative block, provided by CKI expression, and stimulation with RA occur together.

Discussion

Our study demonstrates that induced expression of p16, p21 or p27 in the p16-deficient astrocytoma, U343, in the presence of retinoic acid causes these malignant cells to morphologically resemble primary human astrocytes. The morphological changes in U343 induced by p16, p21 or p27 alone do not resemble normal astrocytes nor does induction with retinoic acid alone. Rather, expression of a predominantly astrocytic phenotype with multiple long cytoplasmic processes occurs only when a strong proliferative block imparted by p16, p21 or p27 expression is accompanied by RA stimulation. Thus, in the absence of a signal from a morphogen (i.e. RA), cell cycle arrest is insufficient to cause U343 cells to resemble primary astrocytes.

It is now well established that cell cycle arrest is associated with CKI-dependent inhibition of cdk activity. Cell cycle arrest is thought to be a requirement for terminal differentiation. Ectopic expression of CKI's in undifferentiated cells can lead to the limited expression of differentiation markers or to morphologic changes of the differentiated phenotype. For example, Vitamin D_3 treatment of U937 leukemia cells causes induction of p21 and p27 mRNA followed by expression of mRNA for macrophage markers (Liu *et al*., 1996). Transfer of p21 or p27 into undifferentiated U937 cells causes an increased expression of CD11b+ and CD14+ cells, suggesting that CKI expression alone is sufficient to induce differentiation in these cells. However, whereas nearly 100% of U937 cells express CD11b+ and CD14+ after vitamin D3 treatment, only 20–35% express these markers after p21 or p27 transfer, and 30–45% do so after co-transfection with p21 and p27. Similarly, DMSO treatment of mouse neuroblastoma cells causes an increase in p27 expression, a shift of pRB to the hypophosphorylated form, and morphologic differentiation (Kranenburg *et al*., 1995). Transfection of p27 into these undifferentiated cells, however, results in only 50% of the cells undergoing a similar morphologic change suggesting that induction of CKI expression alone is inefficient at causing phenotypic differentiation.

It is also clear from our study, however, that RA treatment alone of U343 cells only weakly causes a change in morphology of these cells. We suggest that RA-treated U343 cells may represent an intermediate phenotype. The transition to a phenotype resembling primary astrocytes requires a strong block to cell cycle progression normally imparted by $p16^{Ink4a}$. Since U343 cells are $p16^{Ink4a}$-deficient, only a potent block to proliferation imparted by the induced expression of p16, p21 or p27 causes these cells to acquire the astrocytic phenotype.

We confirmed that the architecture of the CKI-induced and/or RA-treated cells resembled primary astrocytes by examining the arrangement of GFAP, vimentin and actin. The disorganized state of these structural proteins is radically altered in response to

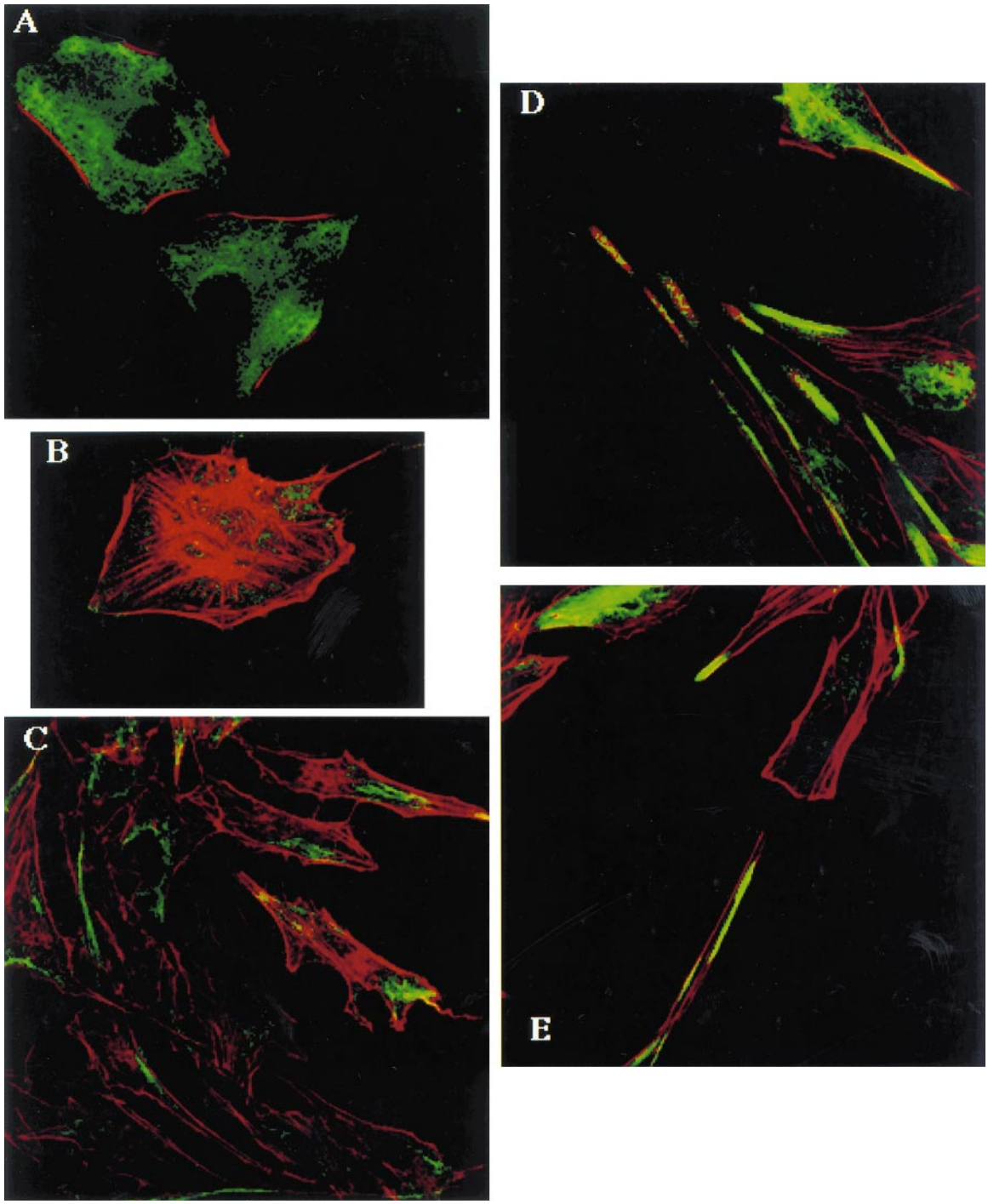

Figure 9 Vimentin and actin staining in U343 cells and primary astrocytes. (**a**) Control U343 astrocytoma cells with typical polygonal morphology. Vimentin immunoreactivity is present in a fine trabecular pattern throughout the cytoplasm, and actin is distributed beneath the surface of the cell membrane. Immunofluorescence confocal microscopy, ×470. (**b**) p16-induced U343 astrocytoma cells. A typical large flat cell is observed. Vimentin immunoreactivity is sparsely dispersed throughout the expanded cytoplasm, but actin is expressed in radial arrays from the cell nucleus reminiscent of stress fiber formation ×470. (**c**) RA-treated U343 astrocytoma cells. The cells have become broadly bipolar, vimentin is found throughout the cytoplasm, and actin is expressed in a filamentous pattern in the cell cytoplasm, ×380. (**d**) RA-treated, p16-induced U343 astrocytoma cells. Specifically, fine actin filaments are seen extending into the long processes that form in these cells. Vimentin, originally confined to the cytoplasm in a perinuclear pattern, is now observed at the tips of the processes of these cells. Vimentin is also localized to a region in the cell body in these RA treated, p16-arrested astrocytomas, this localization being apparently discontinuous with the vimentin at the tips of the processes. The pattern of staining for vimentin and actin in p16-induced, RA-treated U343 cells resembles their staining pattern in normal, primary human astrocytes, ×600. (**e**) Primary human astrocytes in culture. In primary cultured astrocytes, vimentin is also localized to the tips of the processes which extend from the cell bodies and, discontinuously, in the cytoplasm in a discrete area. Actin is also highly organized in these astrocytes, filaments seen extending into the long processes. Multiple long, tapering cytoplasmic processes are seen which stain intensely for vimentin, ×600

CKI-mediated cell cycle arrest. In fact, in data we have not shown, the phosphorylated form of GFAP, which can be detected in both the nuclear and cytoplasmic compartments of U343 cells, specifically disappears from the nuclear compartment upon CKI expression. These data and those described above clearly demonstrate that the activity of the cell cycle machinery can affect cellular architecture and influence the organization of specific cytoskeletal components. The most dramatic reorganization of an intermediate filament was observed for vimentin. Slight reorganization of vimentin occurs in response to RA treatment or CKI expression alone. However, when both signals are provided, vimentin localizes to the tips of the newly formed processes in these cells. This arrangement of this intermediate filament is indistinguishable from its subcellular location in primary human astrocytes. Thus, we conclude that an astrocytic phenotype can be induced in malignant U343 cells when provided with both a strong proliferative block and a morphogenic signal. It will be interesting to determine if the relocalization of vimentin occurs in response to reorganization or expression of, as yet, unidentified factors which promote process outgrowth and/or attachment, such as neural adhesion molecules or integrins.

Materials and methods

Cell culture

The well characterized U343MG-a (U343) malignant astrocytoma cell line was established from a primary malignant astrocytoma in an adult. This particular cell line is a subclone of the original tumor that stably expresses the astrocyte differentiation marker, glial fibrillary acidic protein (GFAP). U343 grows adherently in α-MEM supplemented with 10% fetal bovine serum and penicillin/streptomycin/fungizone (Gibco BRL, Gaithersburg, MD, USA). A culture of primary astrocytes was established from a cortical resection of human brain performed due to a seizure disorder.

For differentiation $2.5-5\times10^5$ cells were plated in 10 cm^2 dishes. All trans retinoic acid (RA) (Sigma, St Louis, MO) was added from 5×10^{-3} M stock solution in 100% ethanol to a final concentration of 5×10^{-6} M. Control cells were cultured in 0.1% ethanol. The medium was changed every other day during the course of all experiments.

Cell proliferation assay

Cell growth was assayed by counting cells at defined intervals. Briefly, cells were trypsinized and resuspended in media, and an aliquot of cells was counted using a hemocytometer. Each count represented an average of five counts on three separate determinations. Cell proliferation assays were repeated in triplicate.

Flow cytometric analysis

To determine the proportion of cells present in a particular cell cycle phase, flow-assisted cell sorting analysis (FACS) of DNA content was performed. Briefly, $0.2-1\times10^6$ cells were trypsinized, washed in phosphate buffered saline (PBS), and resuspended in ice cold 80% ethanol. Cells were kept at 4°C on ice until propidium iodide (PI) DNA staining was performed. For different samples the concentration of cells was kept equivalent. For staining, fixed cells were resuspended in PI and DNAse-inactivated RNase A (final concentration 1 mg/mL) and were incubated for 30 min at room temperature in the dark. Stained cells were filtered through mesh capped tubes and DNA content was analysed on Becton-Dickinson FACScan. Percent cell cycle phase was determined using Cell Fit software (Becton-Dickinson).

Antibodies

Antibodies to cyclin A, cyclin E, cyclin D1, cdk1, cdk2, cdk4, cdk6, E2F1 and E2F4 were obtained from Santa Cruz Biotech. (Santa Cruz, CA) and to pRB and p16 from Pharmingen (San Diego, CA). α-p21 and α-p27 antibodies were obtained from Upstate Biotechnology Inc. (Lake Placid, NY). Antibodies specific for GFAP were obtained from Dako Inc. (Denmark), and vimentin and phalloidin-rhodamine were obtained from Sigma (St Louis, MO, USA), whereas the phosphorylated GFAP antibody (YC-10) was from Medical and Biological Laboratories Co., Ltd. (Nagoya, Japan).

Western blots

Total cell lysates (10–30 mg) were subjected to SDS–PAGE. Proteins were transferred to polyvinylidene difluoride (Immobilon P) membranes by semi-dry transfer. Blots were rehydrated prior to immunodetection, and then were blocked in 5% skim milk in PBS/0.1% Tween 20 at room temperature for 1 h. Primary and secondary antibody incubations were performed in blocking solution at room temperature for 1 h. Goat anti-rabbit or mouse horseradish peroxidase conjugated secondary antibodies were used at 1 : 5000–1 : 8000 concentrations. Detection was performed using the enhanced chemiluminescence system (ECL, Amersham, Oakville, ON).

Immunofluorescence and confocal microscopy

Glass cover slips with cells from each treatment group were permeabilized with 0.02% triton × 100 for 5 min prior to fixation with 4% paraformaldehyde in 0.1 M phosphate buffer (PH 7.2) for 30 min. They were then washed several times with PBS and the residual aldehyde blocked with PBS containing 0.5% BSA and 0.15% glycine. Following several rinses in PBS with 0.5% BSA, the cells were incubated with a monoclonal antibody against vimentin or the polyclonal antibody for GFAP for 1 h. Rhodamine phalloidin was used for actin staining for 30 min. Specimens were then washed thoroughly with PBS prior to incubation with the secondary antibody, a goat anti-murine or anti-rabbit IgG conjugated to FITC or rhodamine (Molecular Probes, Eugene, OR), for 1 h. After a thorough washing, the coverslips were mounted on glass coverslips with mounting medium (Inova Diagnostics, San Diego, CA). Irrelevant antisera or the omission of primary antibody were used as controls. Specimens were then examined under a Leica TCDS 4D confocal laser scanning microscope. 0.5 mm optical sections were obtained and viewed as single planes. In addition, data sets from each cell were rendered as a stacked perspective of all the optical sections. GFAP stains shown were examined with a Leica immunofluorescence microscope.

Histone H1 and pRB kinase assays

Histone H1 and pRB kinase assays were performed according to the protocol of Matsushime *et al*. (1994). For pRB kinase assays, a human recombinant full length pRB was used as a substrate (QED Advanced Research Technologies Inc., San Diego, CA, USA). This recombi-

nant pRB has also been shown to cause cell cycle arrest when microinjected into cancer cells (Pagliaro *et al*., 1995).

Plasmids and transfection

The tetracycline-repressor gene expression system was used to induce expression of the CKI's, p16, p21 and p27. The pUHD-15-1neo plasmid contains the *E. coli* tetracycline repressor element fused to the VP16 transactivation domain of herpes virus. This fusion protein is driven by a CMV promoter and the vector has the neomycin resistance gene for selection. pUHD15-1neo (25 mg) was transfected into U343 cells using the calcium phosphate method. Clones were selected in 900 μg/mL gentecin (Gibco/BRL) in α-MEM and stable expression of the fusion protein was determined by Western blot analysis of total cell lysates using a polyclonal antisera to VP16 (kind gift of Dr J Ingles, Univ. Toronto). Twenty clones were analysed for VP16 expression and the majority expressed VP16. One clone, which demonstrated high level expression of VP16 (clone 88) was selected for transfection with pUHD10-3. pUHD10-3 contains a multiple cloning site downstream from tandem tetracycline operator sequences and a CMV promoter. Full length human cDNAs of p16, p21 (gifts of D Beach) and p27 (gift of J Massague) were inserted into the multiple cloning site of pUHD10-3, and this plasmid (25 μg) was cotransfected with *pgk*-puro (0.5 μg) for selection of stable lines. These clones were also maintained in 4 μg/mL tetracycline added from a 4 mg/mL stock in 70% ethanol. Puromycin was used for selection at 1 μg/mL, and G418 concentration was maintained at 500 μg/mL.

To induce expression of CKI's, cells were washed three times in PBS, before identical media without tetracycline was added. To screen for CKI expression, total cell lysates were collected and Western blot analysis was performed for p16, p21 or p27. To determine the effect of induction of CKI expression on the growth and morphology of U343 cells, $2-5\times10^5$ cells were plated in 100 mm^2 dishes. The following day, fresh media was placed and cell proliferation assays and flow cytometric analysis were performed as described.

Acknowledgements
The pUHD15-1neo plasmid was a kind gift of Dr S Reed and pUHD10-3 was a kind gift of Dr H Bujard. Human p16 and p21 cDNA were gifts from Dr D Beach and human p27 was a gift from Dr J Massague. Rabbit antisera to VP-16 was a generous gift from Dr CJ Ingels, University of Toronto. This work was supported in part through a grant from the MRC to JTR; through a grant to PAH from the National Cancer Institute of Canada with support from the Canadian Cancer Society and through funds from The Research Institute, The Hospital for Sick Children to JTR. PBD is supported by an NCIC research fellowship with funds provided by the Canadian Cancer Society as well as a research fellowship from the MRC.

References

Caldas C, Hahn SA, da Costa LT, Redston MS, Schutte M, Seymour AB, Weinstein CL, Hrurban RH, Yeo CJ and Kern SE. (1994). *Nature Genet*., **8,** 27–32.

Coats S, Flanagan WM, Nourse J and Roberts JM. (1996). *Science*, *272,* 877–880.

Cobrinik D, Whyte P, Peeper DS, Jacks T and Weinberg RA. (1993). *Genes & Dev*., **7,** 2392–2404.

Dulic V, Kaufmann WK, Wilson SJ, Tlsty TD, Lees E, Harper JW, Elledge SJ and Reed SI. (1994). *Cell*, **76,** 1013–1023.

El-Deiry WS, Tokino T, Velculescu VE, Levy DB, Parsons R, Trent JM, Lin D, Mercer WE, Kinzler KW and Vogelstein B. (1993). *Cell*, **75,** 817–825.

Fero ML, Rivkin M, Tasch M, Porter P, Carow CE, Firpo E, Polyak K, Tsai L-H, Broudy V, Perlmutter RM, Kaushansky K and Roberts JM. (1996). *Cell*, **85,** 733–744.

Gossen M and Bujard H. (1992). *Proc. Natl. Acad. Sci. USA*, **89,** 5547–5551.

Harper JW, Adami GR, Wei N, Keyomarsi K and Elledge SJ. (1993). *Cell*, **75,** 805–816.

Hengst L, Dulic V, Slingerland JM, Lees E and Reed SI. (1994). *Proc. Natl. Acad. Sci. USA*, **91,** 5291–5295.

Hussussian CJ, Struewing JP, Goldstein AM, Higgins PAT, Ally DS, Sheahan MD, Clark Jr, WH, Tucker MA and Dracopoli NC. (1994). *Nature Genet*., **8,** 15–21.

Ichimura K, Schmidt EE, Goike HM and Collins VP. (1996). *Oncogene*, **13,** 1065–1072.

Jen J, Harper JW, Bigner SH, Bigner DD, Papadopoulos N, Markowitz S, Willson JKV, Kinzler KW and Vogelstein B. (1994). *Cancer Res*., **54,** 6353–6358.

Kamb A. (1995). *Trends Genet*., **11,** 136–140.

Kamb A, Gruis NA, Weaver-Feldhaus J, Liu Q, Harshman K, Tavtigian SV, Stockert E, Day III RS, Johnson BE and Skolnick MH. (1994). *Science*, **264**.

Kiyokawa H, Kineman RD, Manova-Todorova KO, Soares VC, Hoffman ES, Ono M, Khanam D, Hayday AC, Frohman LA and Koff A. (1996). *Cell*, **85,** 721–732.

Kranenburg O, Scharnhorst V, van der Erb AJ and Zantema A. (1995). *J. Cell Biol*., **131,** 227–234.

LaBaer J, Garrett MD, Stevenson LF, Slingerland JM, Sandhu C, Chou HS, Fattaey A and Harlow E. (1997). *Genes Dev*., **11,** 847–862.

Liu L, Lassam NJ, Slingerland JM, Bailey D, Cole D, Jenkins R and Hogg D. (1995). *Oncogene*, **11,** 405–412.

Liu M, Lee M-H, Cohen M, Bommakanti M and Freedman LP. (1996). *Genes Dev*., **10,** 142–153.

Matsuoka Y, Nishizawa K, Yano T, Shibata M, Ando S, Tanabe K, Kikuchi K, Tsuiki S and Nishi Y. (1992). *EMBO J*., **11,** 2895–2902.

Matsushime H, Quelle DE, Shurtleff SA, Shibuya M, Sherr CJ and Kato J-A. (1994). *Mol. Cell Biol*., **14,** 2066–2076.

Nakayama K, Ishida N, Shirane M, Inomata A, Inoue T, Shishido N, Horii I, Loh DY and Nakayama K-I. (1996). *Cell*, **85,** 707–720.

Pagliaro LC, Antelman D, Johnson DE, Machemer T, McCulloch EA, Freireich EJ, Stass SA, Shepard HM, Maneval D and Gutterman JU. (1995). *Cell Growth & Differ*., **6,** 673–680.

Parry D, Bates S, Mann DJ and Peters G. (1995). *EMBO J*., **14,** 503–511.

Polyak K, Kato J, Solomon MJ, Sherr CJ, Massague J, Roberts JM and Koff A. (1994a). *Genes & Dev*., **8,** 9–22.

Polyak K, Lee M-H, Erdjument-Bromage H, Koff A, Roberts JM, Tempst P and Massagué J. (1994b). *Cell*, **78,** 59–66.

Poon RYC and Hunter T. (1995). *Science*, **270,** 90–93.

Resnitzky D, Gossen M, Bujard H and Reed SI. (1994). *Mol. Cell Biol*., **14,** 1669–1679.

Reynisdottir I, Polyak K, Iavarone A and Massague J. (1995). *Genes Dev*., **9,** 1831–1845.

Rutka JT, DeArmond SJ, Giblin JR, McCulloch JR, Wilson CB and Rosenblum ML. (1988). *Int. J. Cancer*, **53,** 3634–3631.

Schmidt EE, Ichimura K, Reifenberger G and Collins VP. (1994). *Cancer Res*., **54,** 6321–6324.

Serrano M, Hannon G and Beach D. (1993). *Nature*, **366,** 704 – 707.
Serrano M, Lee HW, Chin L, Cordon-Cardo C, Beach D and DePinho RA. (1996). *Cell*, **85,** 27 – 37.
Shan B, Chang C-Y, Jones D and Lee W-H. (1994). *Mol. Cell Biol.*, **14,** 299 – 309.
Sherr CJ and Roberts JM. (1995). *Genes & Dev.*, **9,** 1149 – 1163.
Smith EA, Leone G, DeGregori J, Jakoi L and Nevins JR. (1996). *Mol. Cell Biol.*, **16,** 6965 – 6976.
Toyoshima H and Hunter T. (1994). *Cell*, **78,** 67 – 74.
Vairo G, Livingston DM and Ginsberg D. (1995). *Genes & Dev.*, **9,** 869 – 881.
Waldman T, Kinzler KW and Vogelstein B. (1995). *Cancer Res.*, **55,** 5187 – 5190.
Weinberg RA. (1995). *Cell*, **81,** 323 – 330.
Yano T, Taura C, Shibata M, Hirono Y, Ando S, Kusubata M, Takahashi T and Inagaki M. (1991). *Biochem. Biophys. Res. Comm.*, **175,** 1144 – 1151.